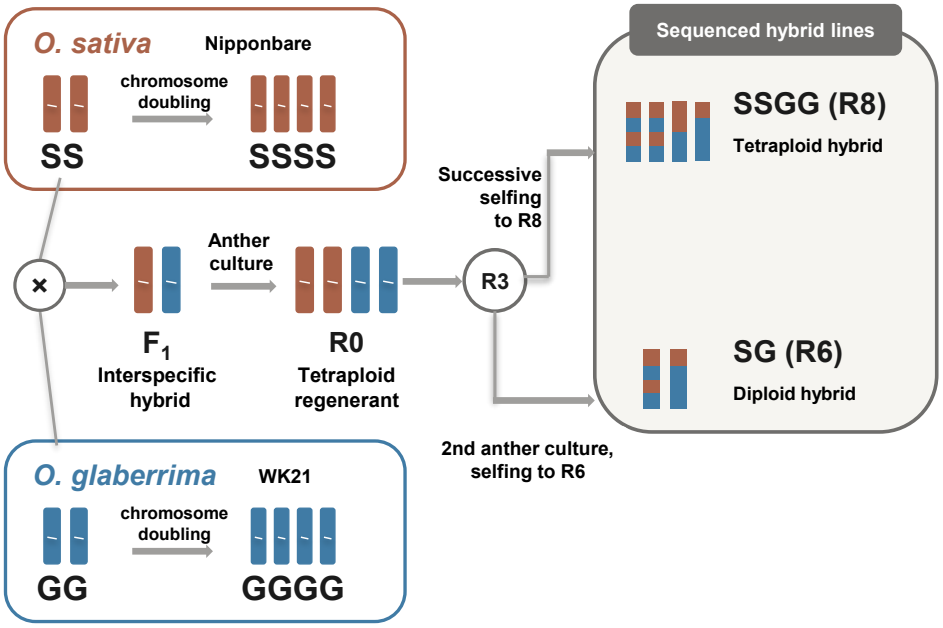


Fig. S1. Origin of the six rice lines analysed in this study.
SS and GG denote Nipponbare and WK21, respectively, and SSSS and GGGG are their autotetraploids. Anther culture of the interspecific F_1 yielded a tetraploid lineage, which was selfed to SSGG (R8). A second anther culture of an R3 plant yielded a diploid lineage, which was selfed to SG (R6). R0 denotes each primary regenerant, with generations counted separately after each regeneration. Only the six coded lines were RNA-sequenced, with three biological replicates each. Bars represent genome sets, with reddish-brown and blue denoting S and G origin, respectively. In the sequenced SG and SSGG lines, the coloured segments schematically illustrate mosaic parental ancestry. Segment lengths and boundaries do not represent actual genomic proportions or exchange breakpoints.

Alt text for Fig. S1
A pedigree diagram connects the diploid parents with their autotetraploids and hybrid lines obtained through anther culture and selfing. Tetraploid SSGG was analysed at R8. Diploid SG was analysed at R6 after a second anther culture from an R3 plant of the tetraploid lineage.

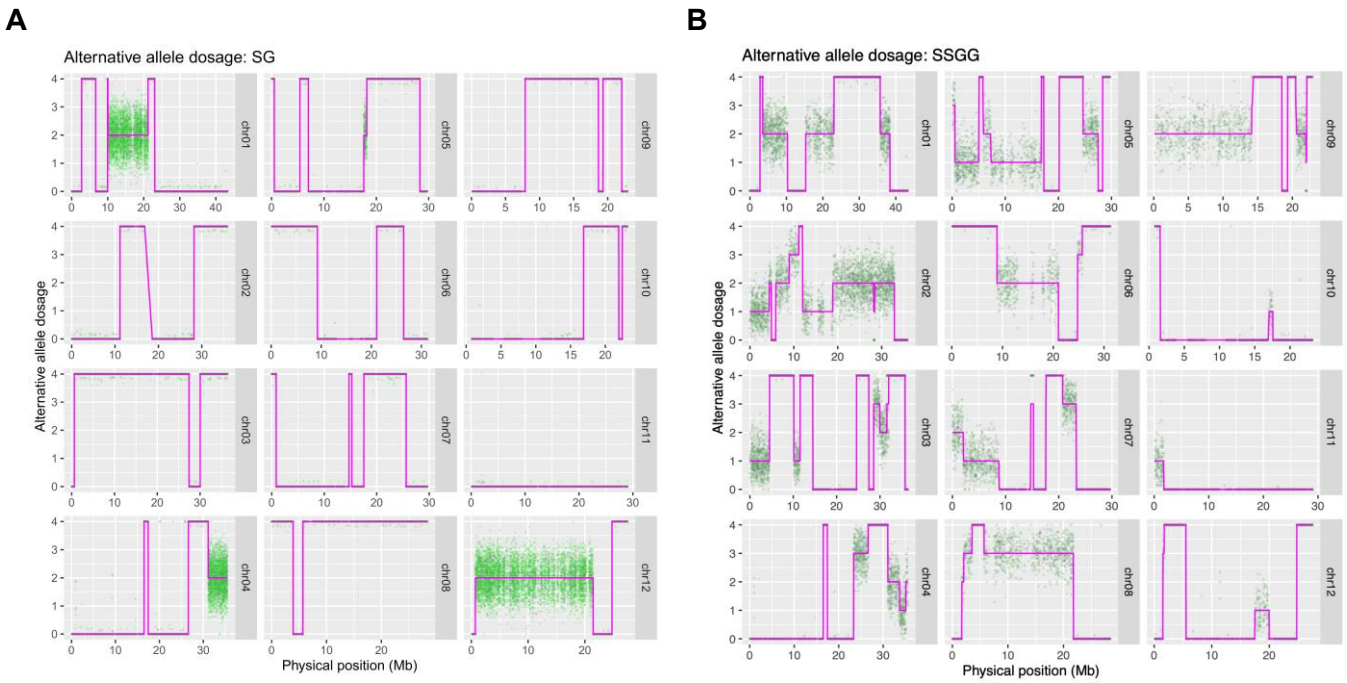


Fig. S2. Distribution of parental genome dosage along the 12 chromosomes of the two interspecific hybrids.

(A) SG; (B) SSGG. The shared 0–4 scale represents G-genome contribution: 0, 1, 2, 3, and 4 correspond to S:G ratios of 4:0, 3:1, 2:2, 1:3, and 0:4, respectively. Diploid SG has inferred dosage states of 0, 2, and 4. A value of 2 denotes equal S/G dosage (Hetero 2). In both panels, green points show observed read ratios and the magenta line shows the inferred dosage state.

Alt text for Fig. S2

Chromosome plots show observed parental read ratios as points and inferred dosage states as stepped lines for SG and SSGG. Parental genomic contributions change along the 12 chromosomes. SG has three inferred dosage classes, whereas SSGG has five.

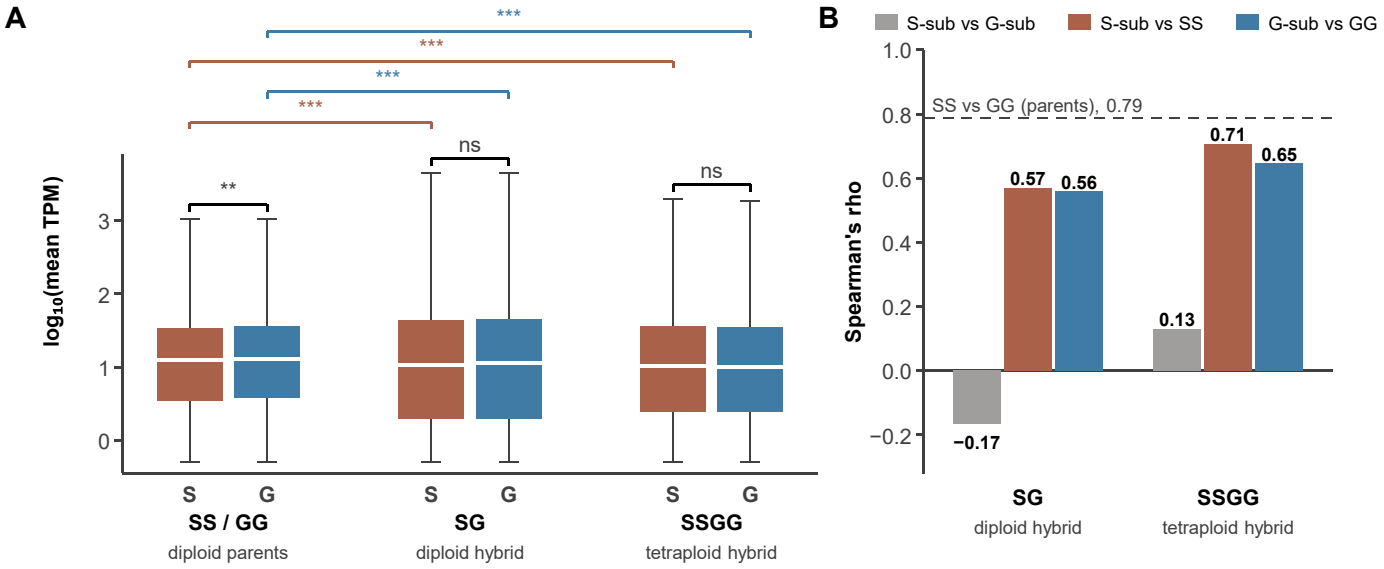


Fig. S3. Expression levels and correlations of S and G genomes or subgenomes in diploid parents and interspecific hybrids.

TPM was normalised within each genome/subgenome and averaged over three biological replicates.

(A) Log_{10}(mean TPM) distributions for genes with mean TPM > 0.5. Gene counts for S/G are 18,591/18,859 in the parents, 13,743/13,363 in SG, and 14,952/14,521 in SSGG. Boxes show medians and quartiles; whiskers extend to values within 1.5 interquartile ranges; outliers are omitted. Black brackets compare S and G within groups; coloured brackets compare hybrid subgenomes with their diploid parents. Two-sided Mann–Whitney U tests (ns, P ≥ 0.05; **, P < 0.01; ***, P < 0.001). Effect sizes were small (rank-biserial |r| ≤ 0.07).

(B) Spearman correlations of mean TPM across the same 21,978 orthologous pairs with mean TPM > 0.5 in at least one of the six genomes/subgenomes in (A). Each bar represents one correlation across gene pairs, not a replicate mean. All correlation tests were two-sided (P < 0.001). The dashed line represents the SS–GG correlation.

Alt text for Fig. S3

Box plots compare log-transformed mean expression of S- and G-derived genes in diploid parents and hybrid lines. Grouped bars show S/G correlations within hybrids and hybrid–parent correlations. A dashed line marks the expression correlation between the two diploid parents.

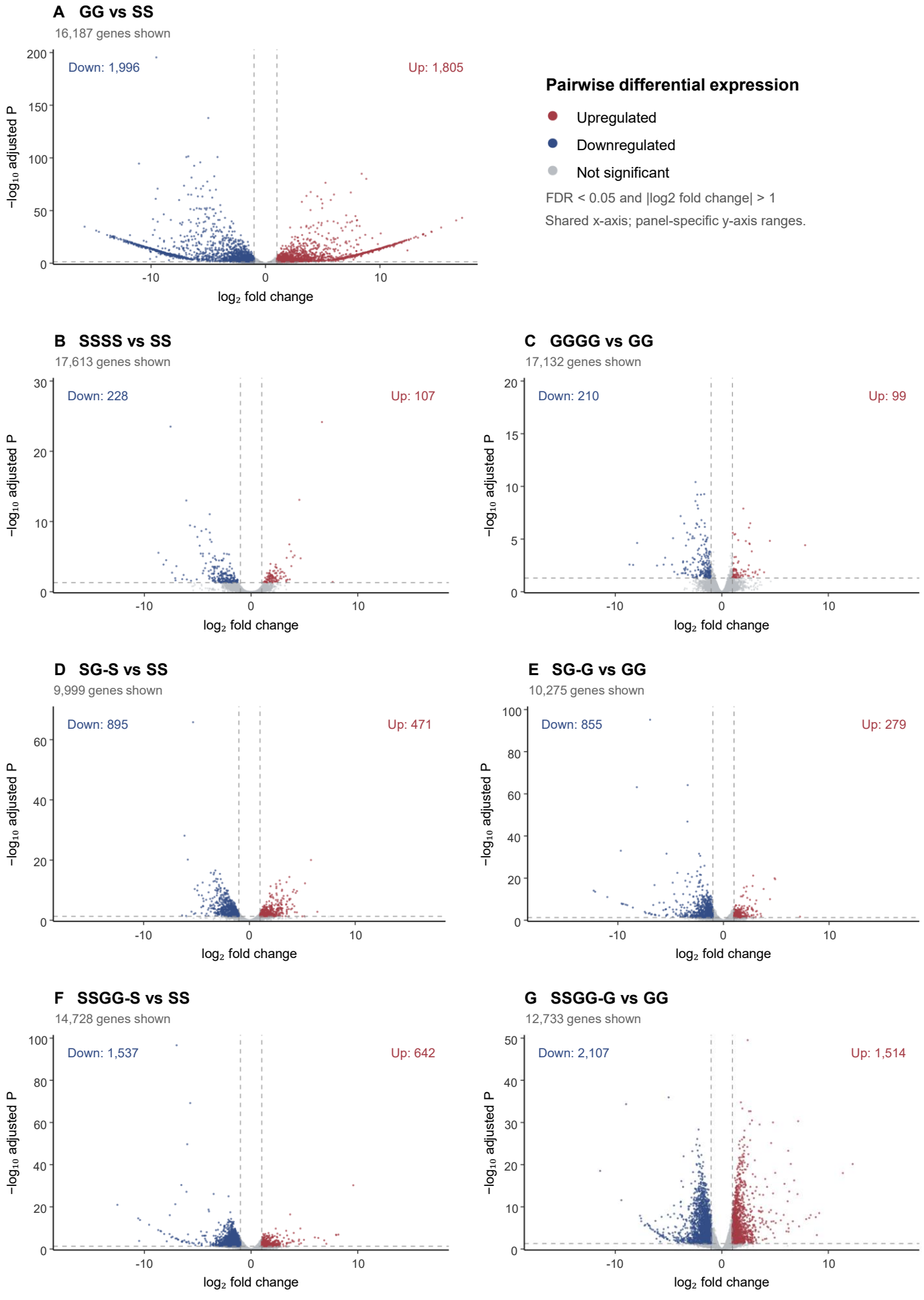

A GG vs SS
16,187 genes shown
Down: 1,996
Up: 1,805
B SSSS vs SS
17,613 genes shown
Down: 228
Up: 107
C GGGG vs GG
17,132 genes shown
Down: 210
Up: 99
D SG-S vs SS
9,999 genes shown
Down: 895
Up: 471
E SG-G vs GG
10,275 genes shown
Down: 855
Up: 279
F SSGG-S vs SS
14,728 genes shown
Down: 1,537
Up: 642
G SSGG-G vs GG
12,733 genes shown
Down: 2,107
Up: 1,514
−log10 adjusted P
log2 fold change
Pairwise differential expression
Upregulated
Downregulated
Not significant
FDR < 0.05 and |log2 fold change| > 1
Shared x-axis; panel-specific y-axis ranges.

Fig. S4. Volcano plots of differential gene expression across seven pairwise comparisons.
(A) GG relative to SS. (B, C) SSSS relative to SS and GGGG relative to GG. (D, E) S- and G-derived genes of SG relative to SS and GG, respectively. (F, G) S- and G-derived genes of SSGG relative to SS and GG, respectively. Each point represents a tested annotation identifier with a finite $\log_2$ fold change and adjusted P-value; the parental comparison uses orthologous transcript pairs. The x-axis shows $\log_2$ fold change for the first-named group relative to the second, and the y-axis shows $-\log_{10}$ adjusted P. Red and blue indicate upregulated and downregulated DEGs, respectively, identified at adjusted $P < 0.05$ and $|\log_2 \text{ fold change}| > 1$; grey indicates genes not meeting both criteria. Dashed lines mark these thresholds. All panels share the same x-axis range, whereas y-axis ranges differ. Labels give the number of plotted identifiers and the upregulated and downregulated DEG counts.

Alt text for Fig. S4
Seven volcano plots show log2 expression fold change against adjusted statistical significance for the parental comparison, two autotetraploid–parent comparisons and four hybrid-subgenome–parent comparisons. Points distinguish upregulated, downregulated and non-significant genes. Axis ranges and gene counts are labelled for each panel.

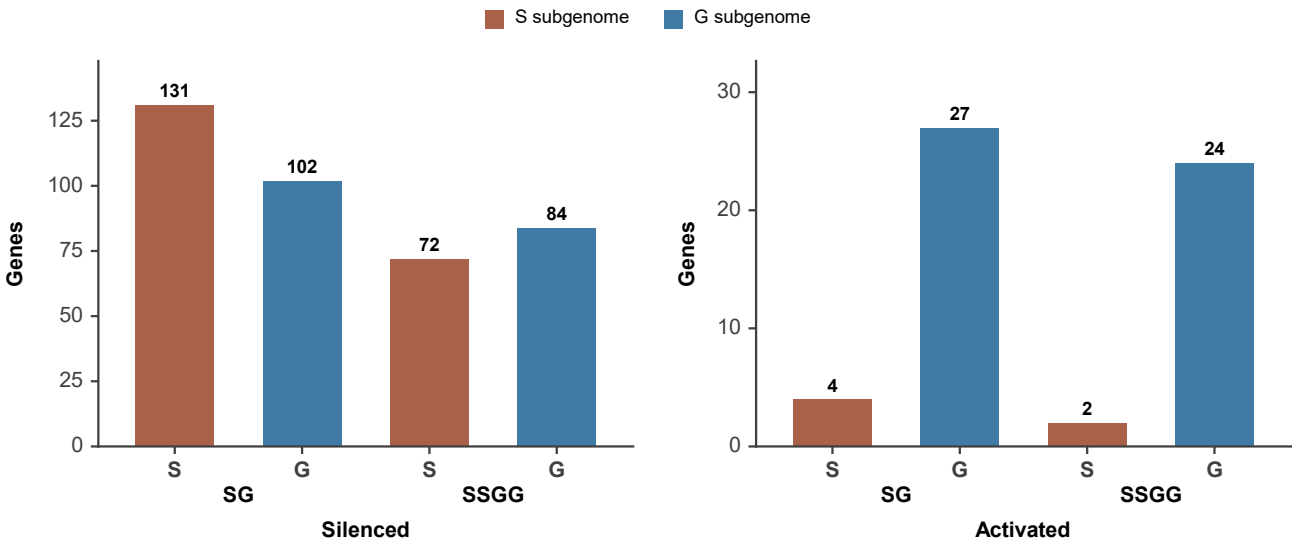


Fig. S5. Gene silencing and activation in dosage-balanced regions of interspecific hybrids.
Bars show gene counts for silencing (left) and activation (right) in the S (reddish-brown) and G (blue) subgenomes of SG and SSGG. Silencing required >10 reads per million (RPM) in all three diploid parent replicates and 0 assigned reads in all three hybrid subgenome replicates. Activation required the reverse pattern. Parental reference gene sets were used for calls in Hetero 2 regions, without restriction to orthologous pairs, separately from DEG calling. Numbers above bars represent gene counts; the two plots have separate y-axes.

Alt text for Fig. S5
Grouped bars compare silenced and activated gene counts for the S and G subgenomes of SG and SSGG. Silenced genes outnumber activated genes in both hybrids. SSGG has lower totals of both silenced and activated genes than SG.

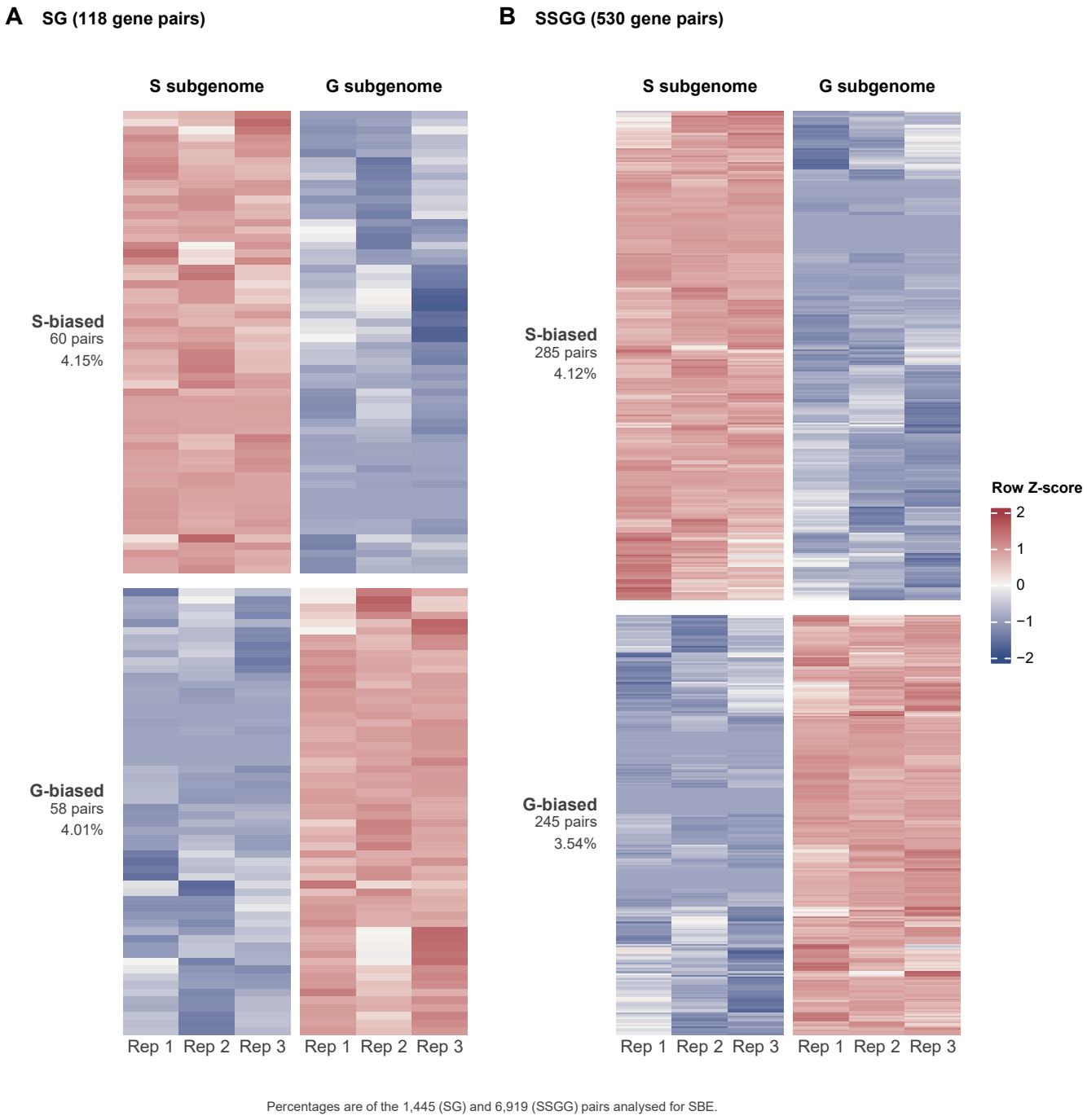


Fig. S6. Expression profiles of gene pairs showing significant subgenome-biased expression in SG and SSGG.

Heatmaps show significant SBE pairs in (A) SG and (B) SSGG. Rows represent orthologous pairs at independent gene loci (118 in SG; 530 in SSGG). The six columns contain three S-copy replicates followed by three G-copy replicates. Colours show row Z-scores of $\log_2$(normalised count + 1): blue, lower; white, row mean; red, higher. Rows are grouped according to bias direction and clustered within groups using Euclidean distance and complete linkage; dendrograms are omitted. Labels provide pair counts and percentages of all analysed dosage-balanced pairs (1,445 in SG; 6,919 in SSGG). The panels represent different pair sets. Plots were generated in R using ComplexHeatmap and circlize.

Alt text for Fig. S6

Two heatmaps show S- and G-copy expression across three replicates for 118 biased gene pairs in SG and 530 in SSGG. Rows are grouped by S-biased or G-biased expression. Colours represent standardised expression within each gene pair.

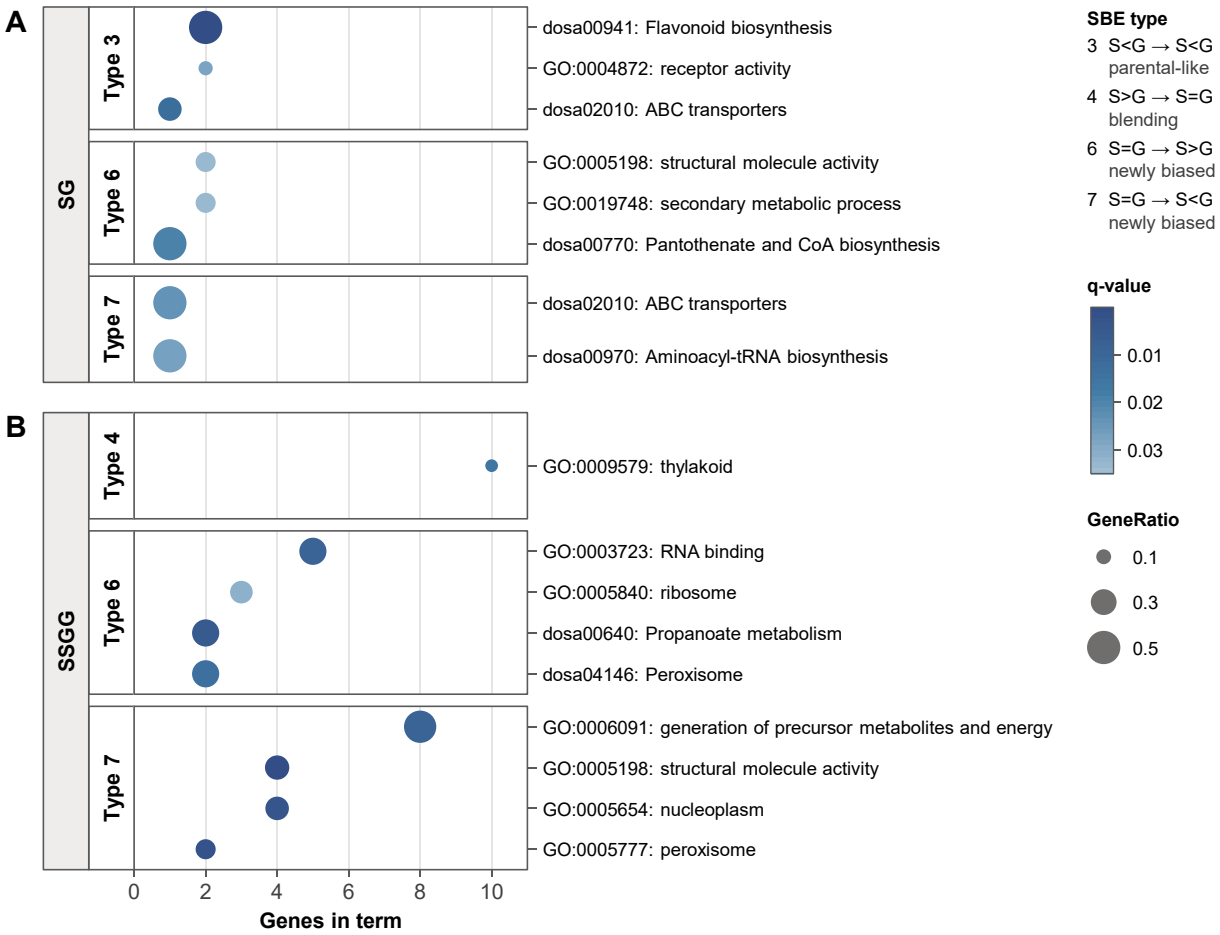


Fig. S7. Gene Ontology and KEGG enrichment in subgenome-biased expression categories.
(A) SG; (B) SSGG. Category numbers follow Supplementary Table S3. Only types with at least one enriched term ($q < 0.05$) are shown: 3, 6, and 7 in SG; 4, 6, and 7 in SSGG. The x-axis gives genes assigned to each term in the corresponding enrichment output. Point size represents reported GeneRatio and colour its *q*-value. GO identifiers begin with GO: and KEGG identifiers with dosa.

Alt text for Fig. S7
Dot plots show selected enriched Gene Ontology terms and KEGG pathways for expression-bias categories in SG and SSGG. Horizontal positions indicate gene counts, dot sizes indicate gene ratios, and colour shades indicate q values.

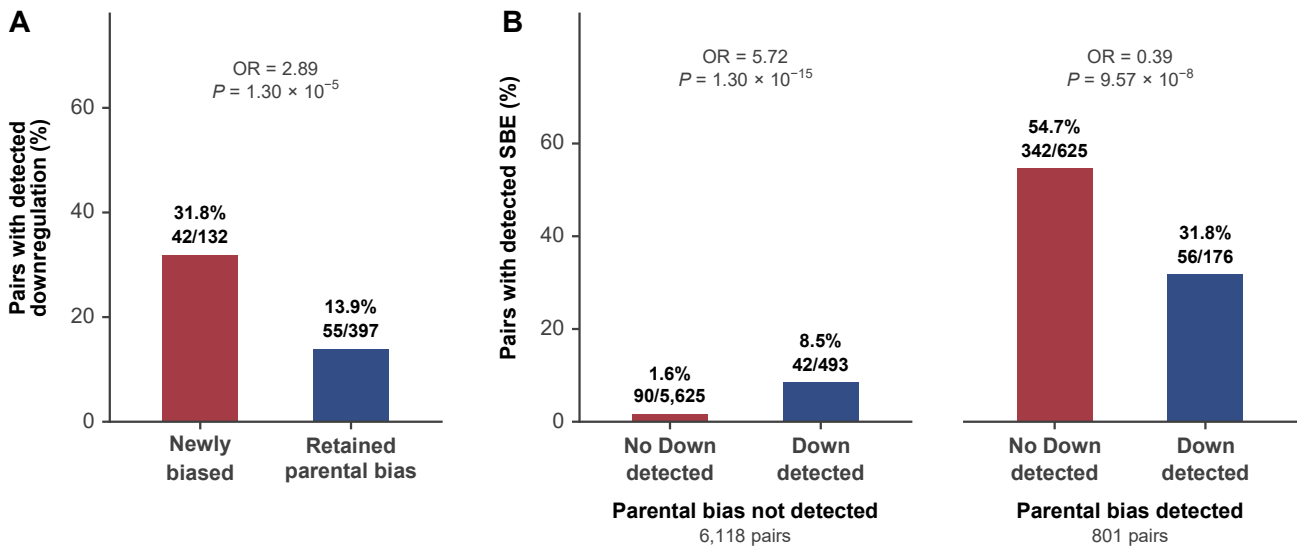


Fig. S8. Associations between downregulation and subgenome-biased expression in SSGG.
A pair was classified as downregulated when at least one copy was significantly downregulated relative to that in its corresponding diploid parent. (A) Downregulation frequencies in Newly biased pairs (red) and pairs retaining the parental bias direction (blue); the Reversal pair is excluded. The odds ratio (OR) compares downregulation odds in Newly biased versus retained-bias pairs. (B) SBE frequencies without (red) or with (blue) detected downregulation, stratified by the absence (6,118 pairs) or presence (801 pairs) of parental bias. All 6,919 dosage-balanced pairs, including the Reversal pair, are included. OR compares SBE odds with versus without downregulation. The labels provide numerators, denominators, and percentages. Two-sided Fisher's tests supply ORs and raw P-values; the two Benjamini–Hochberg-adjusted P-values in (B) are 2.60×10^{-15} and 9.57×10^{-8}, respectively. Not detected includes absence from significant-gene lists due to low-count prefiltering.

Alt text for Fig. S8
Bar charts compare downregulation frequencies in Newly biased and retained-bias pairs, then compare subgenome expression bias with and without downregulation in two parental-bias groups. The association is positive when parental bias is undetected and negative when parental bias is present.

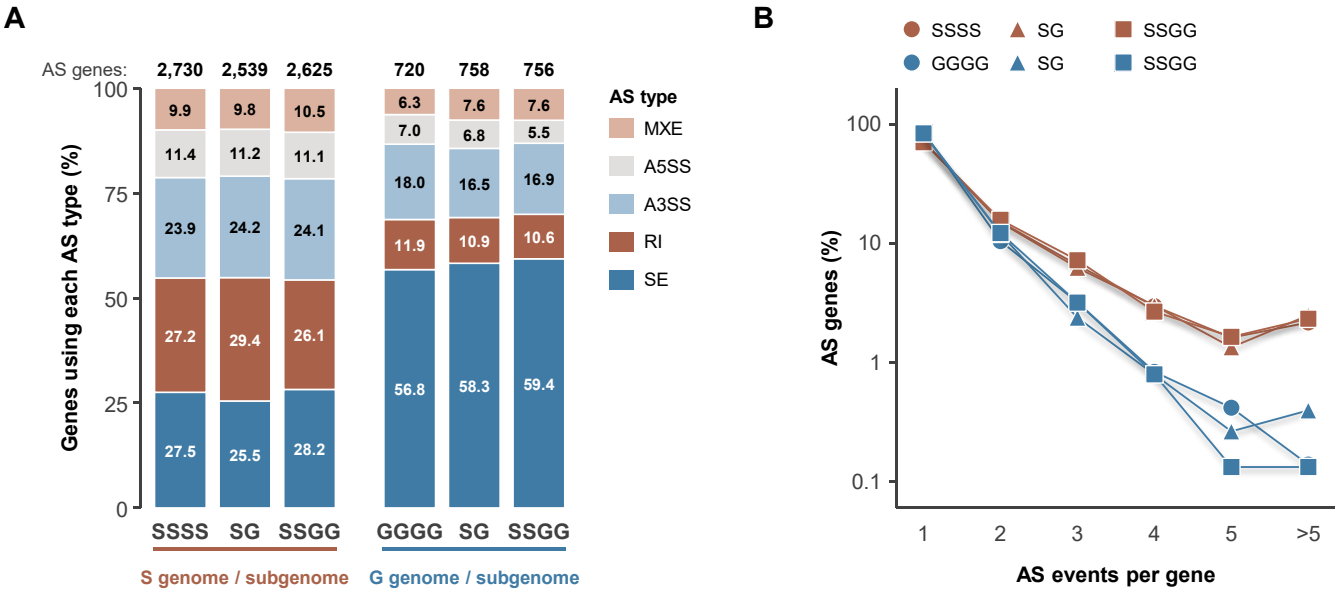


Fig. S9. Gene-level composition of alternative splicing in parental autotetraploids and interspecific hybrids.

AS required 0.05 < mean percent spliced-in (PSI) < 0.95 across three biological replicates.

(A) Gene–AS type associations. Each gene is counted once per detected AS type, so genes with multiple types contribute to multiple segments. Segment percentages reflect all gene–AS type associations, whereas numbers above bars are distinct AS gene counts.

(B) Percentages of distinct AS genes with one, two, three, four, five, or more than five events. Each gene contributes to one class; the denominator is all distinct AS genes in the group. The y-axis is logarithmic.

Alt text for Fig. S9

Stacked bars summarise gene–splicing-type associations in autotetraploids and hybrid subgenomes. Line plots show detected event counts per gene on a logarithmic percentage scale. Most genes have one event; S-derived genes more often have three or more events than G-derived genes.

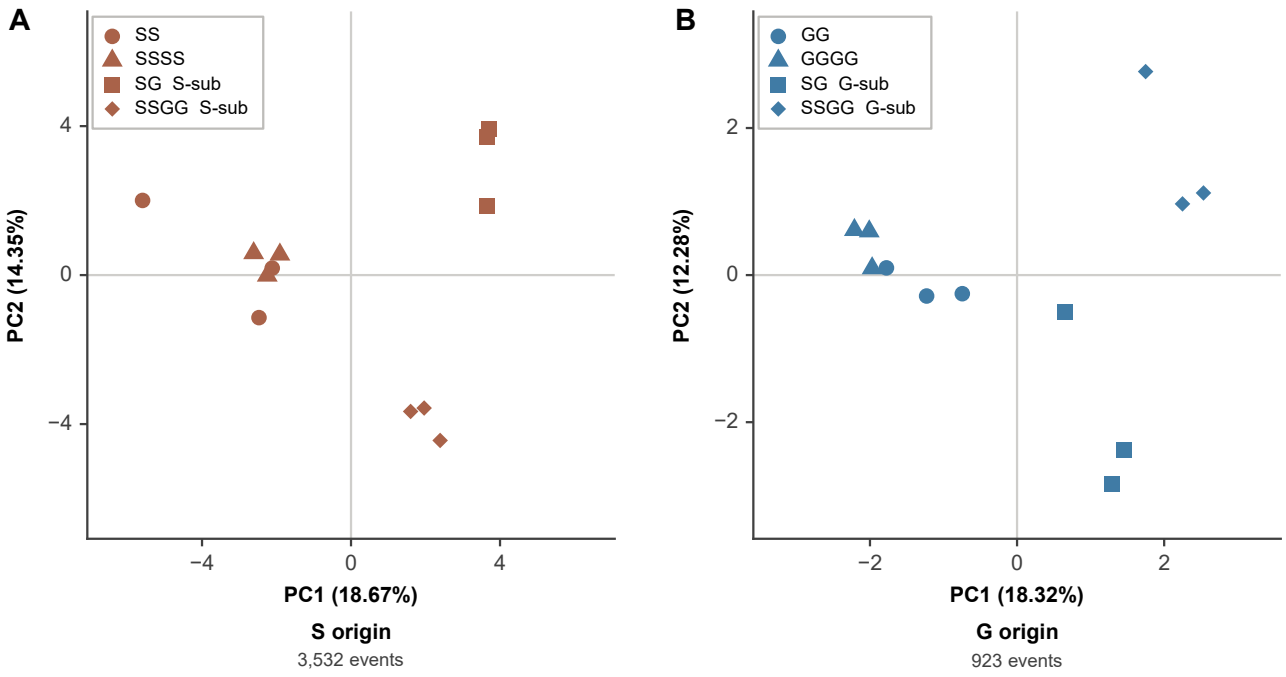


Fig. S10. Principal component analysis of percent-spliced-in (PSI) profiles.
(A) S-origin group; (B) G-origin group. Each panel contains the diploid parent, autotetraploid, and corresponding subgenomes of SG and SSGG, with three biological replicates each. Each point represents one replicate. Analyses used 3,532 S-origin and 923 G-origin events with complete replicate PSI and 0.05 < mean PSI < 0.95 in at least one genotype, irrespective of DSE significance. Each parental replicate is represented once. Event-centred PSI values were analysed without scaling to unit variance; axis percentages indicate explained variance.

Alt text for Fig. S10
Principal component plots compare splicing-inclusion profiles for S-origin and G-origin events. In each group, the first component mainly separates hybrid profiles from diploid parents and autotetraploids. The second component separates the diploid hybrid SG from the tetraploid hybrid SSGG.

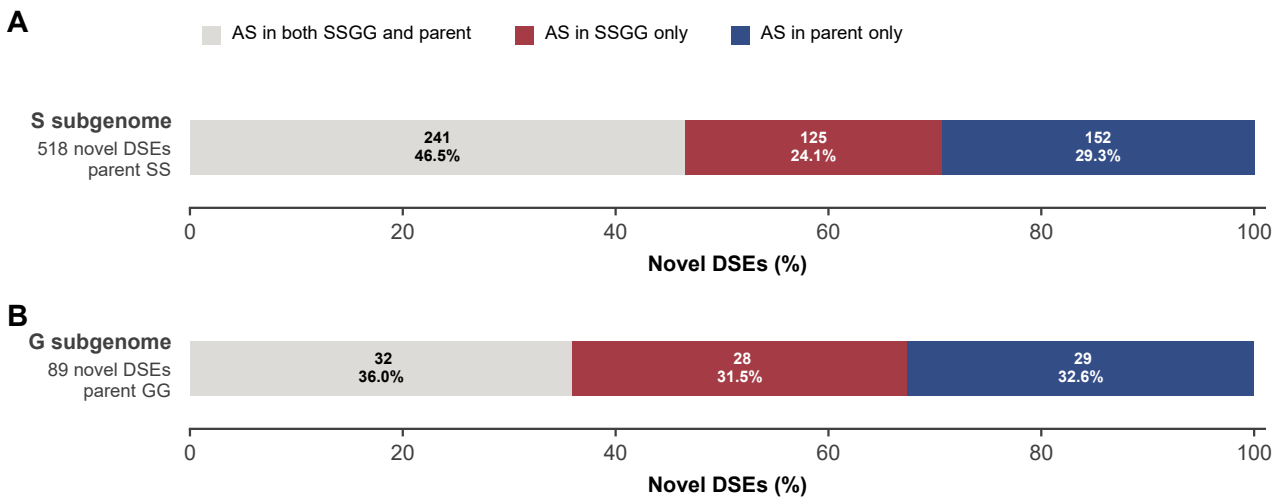


Fig. S11. Alternative splicing states of Novel DSEs in SSGG and their corresponding diploid parents. (A) S subgenome versus SS (518 events); (B) G subgenome versus GG (89 events). Novel follows Fig. 4C: DSEs detected in SSGG, but not SG or the corresponding autotetraploid, each relative to its diploid parent. This does not imply newly created splice sites. Grey indicates AS in both genotypes, red only in SSGG, and blue only in the parent, based on 0.05 < mean PSI < 0.95 across three biological replicates. When AS was detected in only one genotype, one splice form predominated in the other. All events were nevertheless significant DSEs (FDR < 0.05). Labels provide counts and percentages of all Novel DSEs in each subgenome; rounding may prevent totals of exactly 100%.

Alt text for Fig. S11

Stacked bars divide SSGG-specific differential-splicing events by whether alternative splicing is detected in both SSGG and its parent, only in SSGG, or only in the parent. Separate bars summarise 518 S-derived and 89 G-derived events.

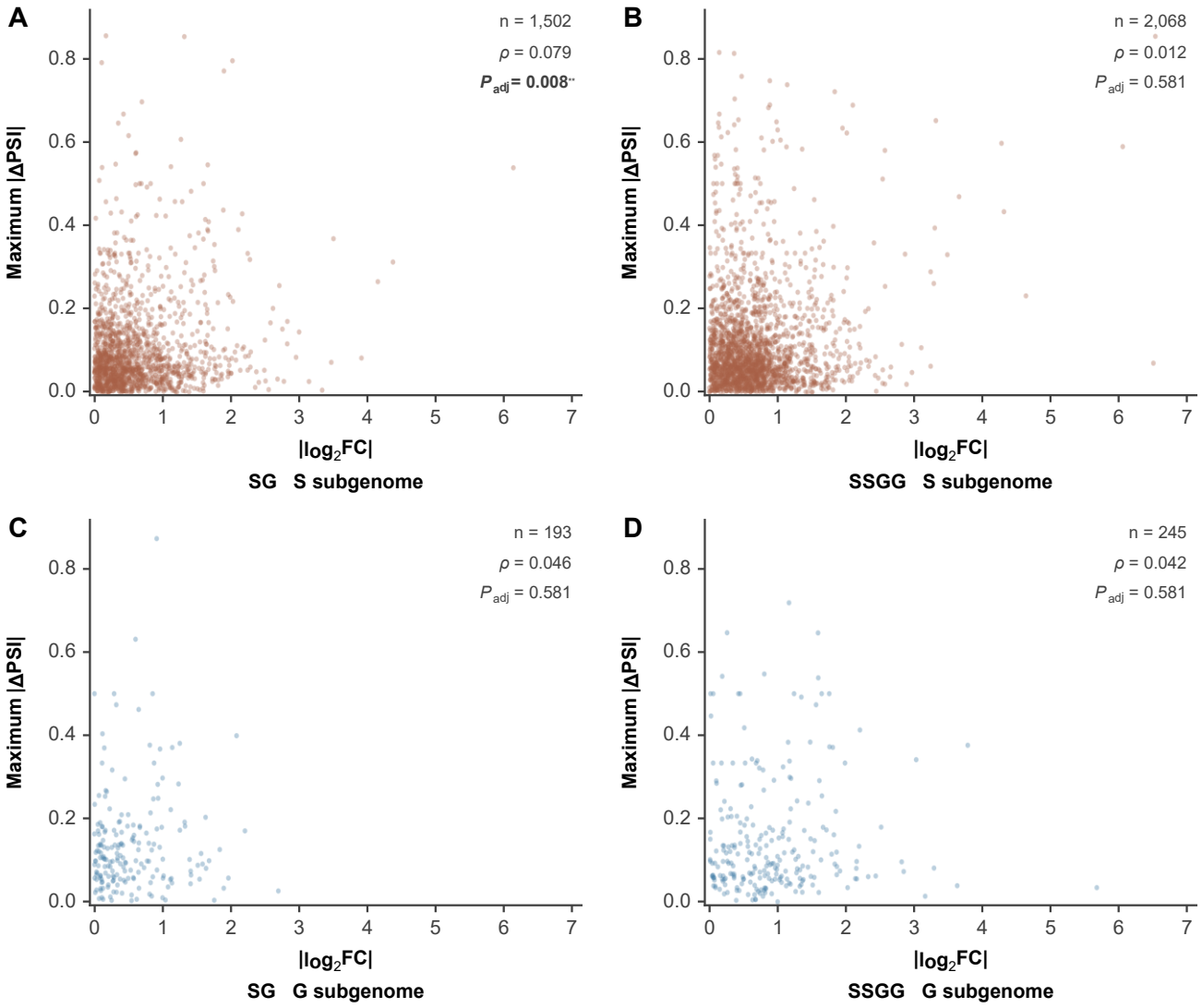


Fig. S12. Associations between the magnitudes of gene expression and alternative splicing changes in SG and SSGG.

(A, B) S subgenomes of SG and SSGG versus SS; (C, D) G subgenomes of SG and SSGG versus GG. Each point is a gene with valid expression and AS results, regardless of DEG/DSG significance. The x-axis is the absolute expression $\log_2$ fold change. The y-axis is the maximum absolute hybrid–parent difference in mean percent spliced-in (PSI), or |ΔPSI|, across all tested AS events of that gene, including non-significant events. Sample sizes count genes, not events: 1,502, 2,068, 193, and 245 in (A–D). Panels show Spearman's ρ and P-values adjusted across the four two-sided tests using Benjamini–Hochberg correction. Bold type and ** indicate an adjusted P-value < 0.01.

Alt text for Fig. S12

Four scatter plots compare absolute log2 fold changes in expression with maximum absolute changes in splicing inclusion for S- and G-derived genes in SG and SSGG. Correlations are weak; only the S-subgenome comparison in SG is significant after multiple-testing correction.